Modelling study to quantify the impact of future climate and land use changes on water resources availability at catchment scale

Muhammad Afzal, Nikolaos Vavlas and Ragab Ragab

ABSTRACT

The focus of this study was to investigate the impact of climate and land-use changes on water resources and to find suitable drought indices to identify the occurrence, frequency and severity of the past and future drought events. The Ebbw catchment, Wales, UK was selected for this study. Data for the 1961–2012 period were used as input to the DiCaSM model. Following model calibration and validation, the model was run with UKCP09 future climate scenarios for three periods (30 years each) up to 2099 under three emission scenarios. The reconnaissance drought index, the standardized precipitation index, soil moisture deficit and the wetness index were able to reproduce the past drought events. The data of UKCP09, simple change factors to temperature (± °C) and rainfall (%) using Joint Probability plot and daily values of the weather generator were input to the model. The projections indicated that the streamflow and groundwater recharge are likely to increase in winter and to decrease in spring, summer and autumn. Under all emission scenarios, the greatest decrease in groundwater recharge and the streamflow is projected in the 2050s and 2080s under high emission scenario. Moreover, under medium and high emission scenarios, severity and frequency of the drought events are likely to be high. Land use change from grass and/or arable to woodland had significant impact on water resources.

Key words | climate change, UKCP09, DiCaSM Hydrological model, Ebbw catchment, water resources, land use change

Muhammad Afzal[†]
Nikolaos Vavlas[‡]
Ragab Ragab (corresponding author)
UK Centre for Ecology & Hydrology (CEH),
Wallingford, Oxfordshire, OX10 8BB,
UK
E-mail: *rag@ceh.ac.uk*

[†]Currently at Cardiff University, Main Building Park Place, Cardiff CF10 3YE, UK
[‡]Currently at Rothamsted Research, West Common, Harpenden, AL5 2JQ, UK

INTRODUCTION

Climate change projections for the UK (Harris *et al.* 2014; Smith *et al.* 2014; Watts *et al.* 2015) and historic trends observed by Alexander *et al.* (2005) and Marsh *et al.* (2007) suggest that it is likely that the UK, in the future, will experience wetter winters and drier summers and might experience more frequent summer droughts. Although there is no universal consensus about the definition of drought (Van Loon and Laaha 2015), an extended period with below average rainfall is considered a 'meteorological drought', this then progresses into an agricultural, hydrological, and socio-economic drought (Byakatonda *et al.* 2018). The general perception is that the UK is not a drought-prone country, however drought events in the UK are not uncommon.

The most severe drought in recent times occurred in the summer of 1976 and affected the whole country, specifically the south-east of England where eight water companies introduced hosepipe bans that affected 15.6 million people and placed water consumers under intense pressure to use water wisely (Taylor *et al.* 2009). Another significant drought event, mainly affecting the north and west of the UK, occurred in 1995 (Marsh 1996). Two successive dry winter and spring seasons led to a drought in 2006 that affected large parts of southern Britain (Marsh *et al.* 2007). The

doi: 10.2166/wcc.2020.117

2010–2012 drought in Wales and the lowland of England was ranked as the most significant one- to two-year drought of the last 100 years (Kendon *et al.* 2013). During the droughts, the rainfall deficiency occurred in the spring, autumn and winter seasons, when normally the replenishment of reservoirs and underground aquifers takes place. Meanwhile, the wetter spells that took place during summer did not increase water resources availability due to higher water losses by evapotranspiration during this time of the year (Grover 2015). Marsh *et al.* (2007) had already pointed out that the UK water reservoirs refill and groundwater recharge occurs during the winter and spring months and that a decrease in rainfall during that time would put extra pressure on water supplies.

Some modelling studies predict higher temperatures, drier summers and wetter winters, and expect that this would be likely to cause a reduction in water resources availability (Arnell 2011). Weatherhead and Knox (2000) reported an increased trend in public water demand in the UK during the past droughts. Future climate change might lead to insufficient water resource availability during drought periods (Rio *et al.* 2018). The most recent drought of summer and winter 2018 is a stark reminder of the past and begs for better preparedness for the future. The year 2018 was considered as one of the hottest and driest years in Europe which resulted in significant drought risk in central and northern Europe which had a large impact on agriculture, ecosystems and society (Hartick *et al.* 2019).

Historic droughts using over 100 near-natural catchments using Standardised Streamflow Index (SSI) across the UK are summarised in Barker *et al.* (2019), and results show the severity of the drought events over the last 125 years in the hydrological time series. Parson *et al.* (2019) compared indices and periods to predict agricultural drought impacts in the UK using two of the most commonly used drought indices Standardized Precipitation Index (SPI) and the Standardized Precipitation Evapotranspiration Index (SPEI) for the period 1975–2012. They found that the SPEI is the best indicator to predict the probability of drought impacts on agriculture in the UK. Although some focus has been given in the previous studies to study the historic drought risk using limited drought indices, less focus has been given to applying a wide range of drought indices in addition to SPI/SPEI or SSI which has broader implications to predict the meteorological, agricultural and hydrological drought under current and future climate conditions.

The risk of seasonal water shortage is especially relevant to areas where agriculture and tourism are important components of the economy. Although several studies of the historic droughts across the UK were carried out at national or regional scale, not much attention was given to the catchment scale and less focus has been given to finding drought indices at local scale that could be useful for local communities such as farmers, fishing industry, allotments society and tourism. Also, little work has been carried out to study the impacts of climate change on possible future change in land use at catchment scale. The aim of this study is to use the Distributed Catchment Scale model, DiCaSM (Ragab and Bromley 2010), to quantify the impact of climate and land use changes on water resources availability in the Ebbw catchment in Wales, UK, and to find suitable drought indices to identify the occurrence, frequency and severity of the past and future drought events.

DATA, THE CATCHMENT AND METHODOLOGY

Catchment description and the data sources

The Ebbw catchment in Wales is situated at Rhiwderin, NRFA reference number 56002, and has a catchment area of 216.5 km^2 (Figure 1). The mean annual rainfall of the catchment is almost equivalent to the average annual rainfall of Wales and is around 1,300 mm per year. The catchment shows a strong north-south gradient in terms of precipitation, and average rainfall in the north can reach up to 1,800 mm/year. The south-side of the catchment receives only 1,000 mm/year. The catchment has a relatively flat wide valley with productive soil, grassland and forests (Figure 2). There are several reservoirs within the catchment boundary, i.e. in the north of the catchment the Shon Sheffrey's reservoir, the Lanton Loch and a few other small reservoirs. They supply water to users within the catchment in winter and spring and run low for the rest of the year. During summer and autumn water supply mostly comes from outside the catchment.

For the modelling study, the catchment was divided into 270 grid squares, each of which has a 1 km^2 area. The model

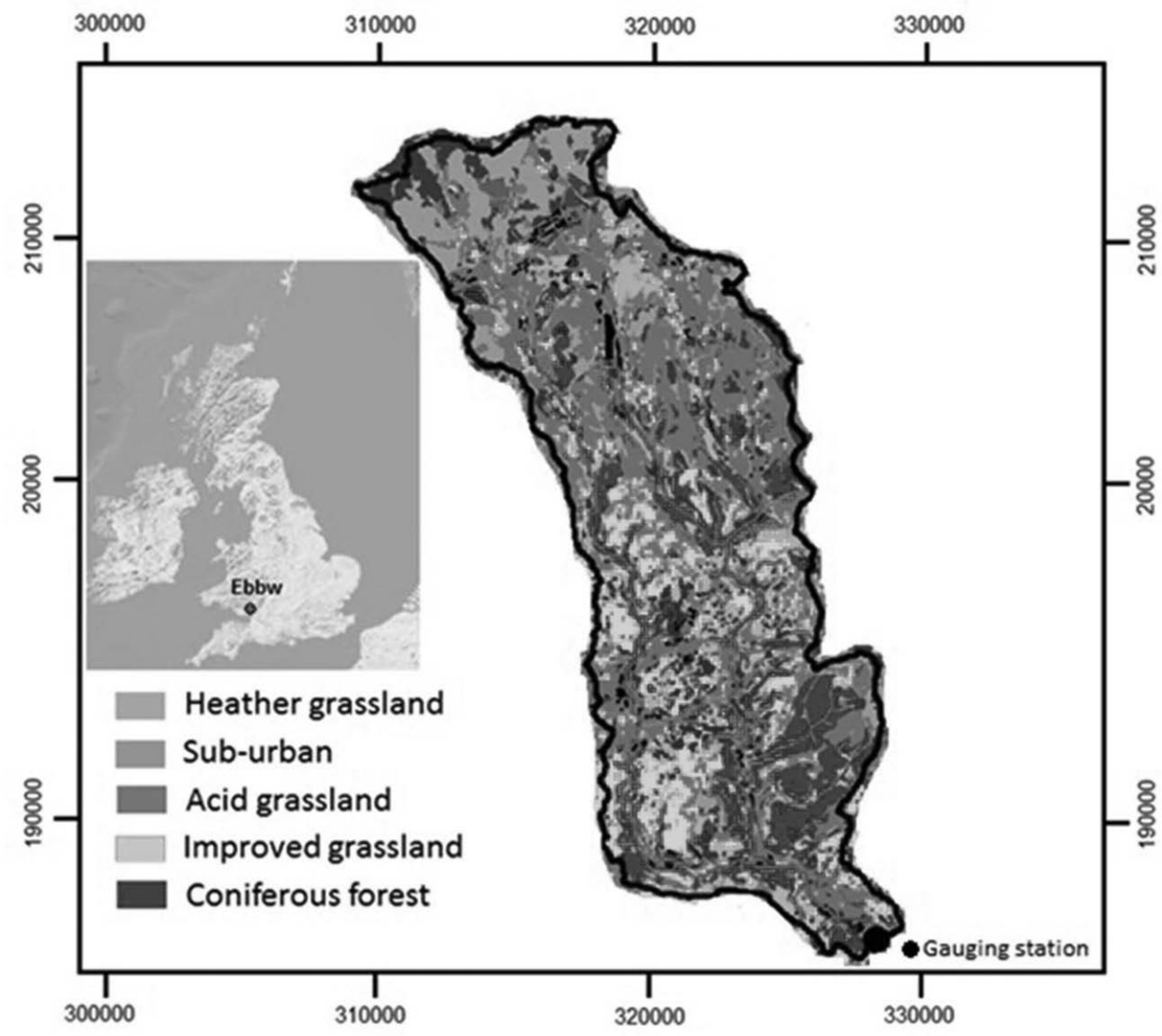

Figure 1 | Ebbw catchment location, catchment boundary, catchment stream route, land use type cover area and the location of gauging station (*Source*: Morton *et al.* 2011).

was run using a daily time step and a spatial scale of 1 km^2 grid square area. The model input requires daily climatic variables including precipitation, temperature, wind speed, daily net radiation and vapour pressure. Climate data were obtained from the Climate, Hydrology and Ecology research Support System (*CHESS*) that accounted for the impact of changes in elevation on climatic data (Robinson *et al.* 2015; Tanguy *et al.* 2016). The development of the Centre for Ecology & Hydrology-Gridded Estimates of Areal Rainfall (CEH-GEAR) data set, 1 km daily Areal rainfall time series were generated across Great Britain for the period 1890–2012 using rainfall interpolation of over 4,400 weather stations, on average one weather station per 49 km^2. Further details are given in Tanguy *et al.* (2016).

The historic continuous climatic variables data were available from 1961 to 2012, whereas the river-flow data were available from 1962 until 2012. The catchment boundary and gauging station location data were available from the Centre for Ecology and Hydrology (Morris *et al.* 1990; Morris and Flavin 1994) and the National River Flow Archive provided data for the daily river flow for the catchment (NRFA 2014). The river characteristic data were

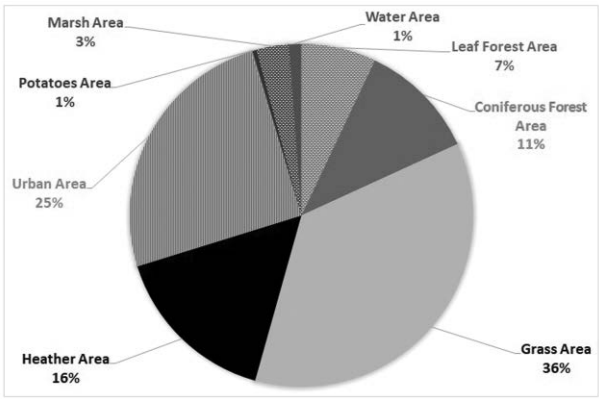

Figure 2 | Current land use in the Ebbw catchment.

collected from the Centre for Ecology and Hydrology, 'Digital Rivers 50 km GB' Web Map Service (CEH 2014). The UK land cover data were obtained from the Centre for Ecology and Hydrology Land Cover Map 2007 (25 m raster, GB) Web Map Service (Morton *et al.* 2011). The soil data was obtained from Cranfield University (1:250 000 Soilscapes for England and Wales Web Map Service). Agriculture census data reveal that less than 5% of the area is cultivated, the main land uses being grassland (36%) and heather (16%). Urban development takes up 25% of the catchment area (Figure 2).

The DiCaSM model

This study applied the Distributed Catchment Scale Model, DiCaSM (Ragab and Bromley 2010; Ragab *et al.* 2010). The model is physically based and considers the commonly known hydrological processes such as rainfall interception, infiltration, evapotranspiration, surface runoff to streams, recharge to groundwater, water uptake by plants, soil moisture dynamics, and streamflow. The model adopts a distributed approach with variable spatial scale (default is 1 km grid square) and requires daily input data of rainfall, temperature, wind speed, vapour pressure and radiation. The model runs on a daily time step, however, if hourly rainfall data is available, the model can run on hourly time step. The model also addresses the heterogeneity of input parameters of soil and land cover within the grid square using three different algorithms. More details about the model can be found in Ragab and Bromley (2010). The model has been successfully applied on catchments in Brazil (Montenegro and Ragab 2010, 2012), in Italy (D'Agostino *et al.* 2010) and in Cyprus (Ragab *et al.* 2010). The results of these studies proved the reliability of the model in simulating the stream flows and in predicting the impact of climate and land use changes on streamflow.

To estimate the model efficiency/goodness of fit, modelled and observed flow data were compared using a number of indices, including the Nash-Sutcliffe Efficiency (*NSE*) coefficient, Equation (1) (Nash and Sutcliffe 1970). The natural logarithm (ln) of *NSE* (Equation (2)) is a variation of NSE and mostly used for low flow conditions (Gupta *et al.* 2009), the value of 1 (or 100%) indicates a perfect match.

$$NSE = 1 - \frac{\sum_{i=1}^{n} (O_i - S_i)^2}{\sum_{i=1}^{n} (\bar{O}_i - \bar{O})^2} \quad (1)$$

$$\ln NSE = 1 - \frac{\sum_{i=1}^{n} (ln\, O_i - ln\, S_i)^2}{\sum_{i=1}^{n} (ln\, \bar{O}_i - \ln \bar{O})^2} \quad (2)$$

where O_i and S_i refer to the observed and simulated river flow data, respectively, and $\bar{O}$ is the mean of the observed data. The calibration procedure consisted of adjusting the streamflow relevant parameters to achieve the best model fit with the latter assessed using the *NSE* and ln *NSE* values for the river flow. In addition, the model performance was also evaluated using the coefficient of determination, R^2 as:

$$R^2 = \left\{ \frac{1}{N} \frac{\sum [(y_0 - \overline{y_0}] \, (\overline{y_s - \overline{y_0}}}{\sigma y_0 - \sigma y_s} \right\} \quad (3)$$

where y_o is the observed value, y_s is the simulated value, N is the total number of observations, $\bar{y}_o$ is the average measured value, $\bar{y}_s$ is the average simulated value, $\sigma\, y_0$ is the observed data standard deviation and $\sigma\, y_s$ is the simulated data standard deviation. The value of this index can range from 0 to 1, with one indicating perfect fit.

Impact of future climate change on water supply systems

To study the impact of future climate change on water supply systems, the UK Climate Projection Scenarios (UKCP09) were used. This study considered three gas emission scenarios (low, medium and high) for three 30-year periods: 2020s (2010–2039), 2050s (2040–2069) and 2080s (2070–2099). The UKCP09 provides monthly, seasonal and annual probabilistic change factors at 25 km^2 grid square resolution for precipitation and temperature. UKCP09 also provides generated daily weather data at a 5 km^2 resolution. The generated data include vapour pressure and sunshine hours, in addition to rainfall and temperature. The sunshine hours were converted into total and net radiation following the methodology of Allen *et al.* (1998). For the initial exploratory analysis, simplified change factors were derived from UKCP09 joint probability central estimates.

The joint probability plot was used to generate seasonal climatic change factors (% change in rainfall and change in temperature, ± °C) as an input to the DiCaSM model. In the weather generator multiple grid cells (cell-size: 5 km^2) were considered in order to totally cover the catchment. For the detailed weather generator simulations, 100 realizations of the daily time series data were generated in order to account for the uncertainty associated with the scenarios and timing of events. A similar approach has been used by other researchers including Cloke *et al.* (2010), Ledbetter *et al.* (2012) and Bastola *et al.* (2012). Table 1 shows the expected joint probability seasonal changes in precipitation and temperature projected under different climate change scenarios relative to the base line data (1961–1990) for the three selected time periods. The seasonal temperature shows an increase in emission scenario and time, particularly in summer and autumn, whereas rainfall decreases in summer and increases in winter.

The daily climatic variables data obtained from the weather generator (WG) were bias corrected using the catchment observation data of the baseline data (1961–1990). The bias correction was conducted using the '*qmap*' package in R statistical tool (Gudmundsson *et al.* 2012).

Selected drought indices

Several drought indices were considered to identify different types of drought:

– The Standardized Precipitation Index, *SPI* (McKee *et al.* 1993) gives the deviation of precipitation from the long-term average precipitation. The SPI is calculated as the difference between monthly precipitation and the mean monthly value divided by the standard deviation. Negative values indicate 'dry periods', positive values indicate 'wet periods'. An SPI value above 2.0 means the conditions are 'extremely wet', 1.5–1.99 'very wet', 1.0–1.49 'moderately wet', −0.99 to 0.99 'near normal', −1.0 to

Table 1 | Probabilistic changes in temperature and precipitation for the Ebbw catchment under UKCP09 climate change scenarios (joint probability) under low, medium and high emission scenarios for the 2020s, 2050s and 2080s (30-years' time periods)

		Low emissions				Medium emissions				High emissions			
		Winter	Spring	Summer	Autumn	Winter	Spring	Summer	Autumn	Winter	Spring	Summer	Autumn
Change in precipitation	2020s	5.0	1.9	-6.3	4.5	5.8	0.6	-12.3	2.8	5.2	1.3	-6.5	4.2
	2050s	10.2	0.9	-17.7	3.2	15.0	0.2	-21.0	3.9	15.0	0.9	-22.6	4.4
	2080s	16.5	1.5	-11.5	3.4	20.0	1.8	-22.0	5.6	22.0	2.5	-34.0	3.5
Change in temperature	2020s	1.0	1.3	1.6	1.5	1.2	1.2	1.8	1.5	1.2	1.2	1.6	1.7
	2050s	1.7	1.6	2.5	2.3	1.8	1.9	2.7	2.6	2.0	2.1	3.0	2.8
	2080s	2.2	2.2	2.5	2.8	2.5	2.7	3.5	3.4	3.0	3.4	4.6	4.4

Time period

Emission Scenarios

−1.49 'moderately dry', −1.5 to −1.99 'severely dry' and −2.0 and less means 'extremely dry' (McKee *et al.* 1993). SPI was used by Michaelides and Pashiardis (2008) in Cyprus, Livada and Assimakopoulos (2007), Karavitis *et al.* (2014) in Greece, and by Al-Faraj *et al.* (2015) in Iran and Iraq.

- The Standardised Precipitation – Evapotranspiration Index, SPEI, considers the potential evapotranspiration in addition to the precipitation and is calculated according to Thornthwaite (1948) as:

$$SPEI_i = P_i - PET_i \tag{4}$$

where $SPEI_i$ is the difference between the precipitation (P) and the potential evapotranspiration (PET) for month, i. The SPEI measures the water surplus or deficit for a specific month. A negative value means the month was drier (evapotranspiration losses were greater than precipitation), a positive value means the month was wetter (precipitation was greater than losses by evapotranspiration), (Tirivarombo *et al.* 2018; Solander and Wilson 2018). SPEI has been applied by Bachmair *et al.* (2018), Kunz *et al.* (2018) and Bento *et al.* (2018).

- The Reconnaissance Drought Index, *RDI*, is calculated using the ratio of precipitation to potential evapotranspiration over a certain period (Tsakiris *et al.* 2007). If the losses by evapotranspiration exceed the rainfall, drier conditions and eventually drought would occur. The RDI is calculated as:

$$a_0^{(i)} = \frac{\sum_{j=1}^{12} P_{ij}}{\sum_{j=1}^{12} PET \text{ or } AE_{ij}} \tag{5}$$

$$RDI_n^i = \frac{a_0^{(i)}}{\overline{a_0}} - 1 \tag{6}$$

$$RDI_{st\,(k)}^i = \frac{y_k^{(i)} - \overline{y_k}}{\hat{\sigma}} \tag{7}$$

where P_{ij} and PET_{ij} are the precipitation and potential evapotranspiration, respectively, of the j_{th} month of the i_{th} hydrological year, which starts in October, $\overline{a_0}$ is the arithmetic mean of the a_0 calculated for the number of years under consideration.

- The adjusted *RDI* is calculated using the net rainfall (this is the gross rainfall minus rainfall interception by the canopy) and the actual evapotranspiration.
- The soil moisture deficit, *SMD,* gives the deviation of the soil moisture from the soil moisture at field capacity. Higher values indicate dry conditions while a value of zero means that the catchment's soil moisture is at field capacity which is optimal soil moisture condition for vegetation growth and for recharge.
- The wetness index, *WI* of the root-zone is the scaled soil moisture and ranges from 0 to 1. It indicates how relatively wet or dry a catchment is over a certain period of time. When the *WI* value is 1, the catchment is at the maximum soil moisture and when *WI* is zero, the catchment is at its minimum soil moisture content. Maximum and minimum soil moisture are based on a long-term record of observed soil moisture.

The SPI, SPEI, RDI, WI and Adjusted RDI are indicators of meteorological or hydrological drought, while the *WI* and *SMD* are used to identify agricultural drought.

RESULTS

Model calibration/validation for the streamflow

In order to use the model for future predictions using UKCP09 scenarios, a successful calibration and validation was necessary to obtain the best set of catchment parameters that would lead to credible predictions. The model was calibrated against the observed streamflow. The following model parameters were fine-tuned: the base-flow index, the stream bed infiltration/leakage, the percentage of runoff routed to stream, the catchment storage/time lag coefficient, the exponent function describing the peak flow, the stream storage/time lag coefficient, and the soil hydraulic parameters. More details about the parameters can be found in Ragab and Bromley (2010). The model optimization process helps in finding the best set of parameters that produce the best match with the observed streamflow values. Figure 3 shows the results of the model calibration period (2000–2003).

The model performed well, both during rainy and dry events, and responded according to the soil hydrology status, i.e. during the soil moisture deficit period, small rainfall events did not generate significant streamflow. The NSE value was over 91% for the calibration and the percentage error was less than 1% (Table 2). The validation process carried out over ten-year periods between 1970 and 2010 is shown in Figure 4. The model performed very well during the 1970s drought decade. The overall model performance over the whole period, 1961–2012, was extremely good (NSE = 87%). The full results are shown in Table 2. The correlation between the observed and simulated flow for different time periods is shown in Figure 5. The figure shows the model's capability to reasonably predict streamflow both during the model calibration and validation periods. The successful calibration and validation proved the reliability of model parameters for further application using UKCP09 scenarios.

Model application to identify the historic drought events

Before using the model for future prediction, it is essential to check first if the model is able to reproduce the past drought events. The results of the SPI and SPEI for the Ebbw catchment showed that the SPI and SPEI drought indices identified all the past drought events that took place in the

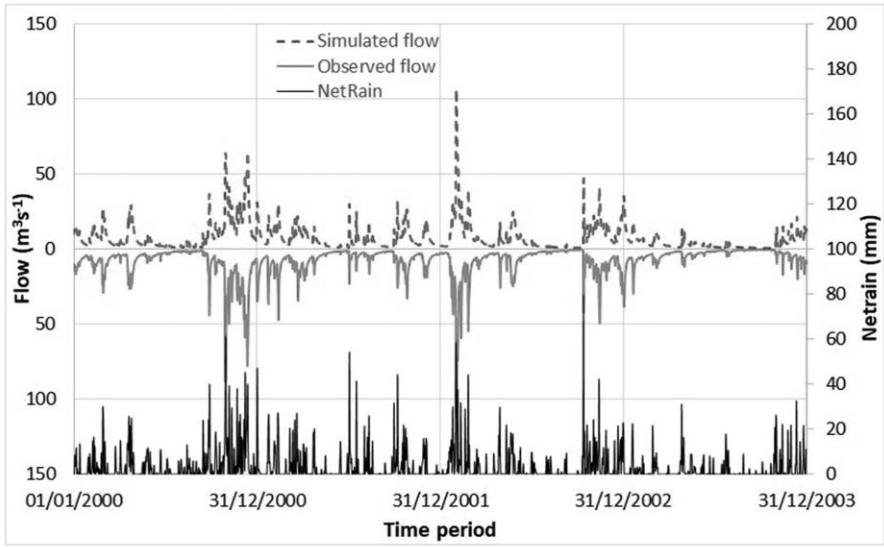

Figure 3 | Ebbw catchment model calibration during the 2000–2003 period.

Table 2 | Ebbw model performance during the calibration and validation stages

Periods	NSE %	Ln NSE %	R^2	Square root of R^2	Modelled flow, m^3s^{-1}	Observed flow, m^3s^{-1}	% Error
2000–2003*	*91*	*88*	*0.92*	*0.96*	*7.19*	*7.23*	*– 0.55%*
1971–1980	87	82	0.88	0.94	6.7	6.53	2.56
1981–1990	86	79	0.87	0.93	7.11	7.49	– 5.02
1991–2000	90	84	0.91	0.95	7.38	7.78	– 4.52
2001–2010	89	80	0.89	0.94	6.74	7.03	– 4.09
1961–2012	87	82	0.88	0.93	6.98	7.21	– 3.17

*Calibration period. %**average daily streamflow of the period.

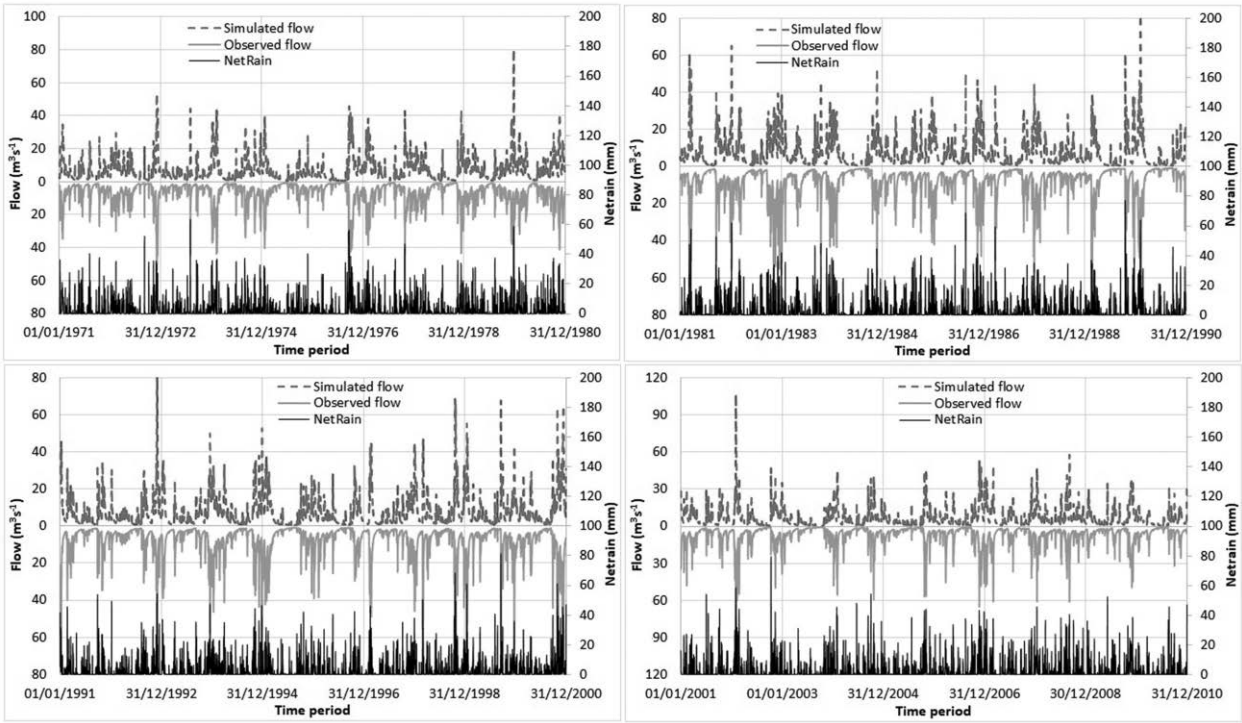

Figure 4 | Ebbw model validation for the periods 1971–1980, 1981–1990, 1991–2000 and 2001–2010.

catchment from the 1961 to 2012 period (Figure 6). As the evapotranspiration calculation in the model is dependent on climatic data as well as on soil and plant parameters, the *SPEI* would be better in representing the severity of the drought. Over the 52-year study period, both the *SPI* and *SPEI* indices identified all the past drought events. Both indices crossed over the 'extremely severe' drought level during the 1970s, a drought that affected all of the UK, as well as large parts of Europe. The more regional droughts of the early 1960s and the one in 1995 were also picked up as being 'severe' by both indices. Similar results were obtained by Phillips and McGregor (1998) who classified the early 1960s drought as a class-1 drought as SPEI was equal to or less than −4.0.

Figure 7 shows the comparison between the RDI and the Adjusted RDI. Both indices identified the past drought events that occurred during the 52-year study period but the Adjusted RDI showed slightly different severity levels, especially during the extreme drought events. The RDI has been used in several studies including studies in Greece (Vangelis *et al.* 2013) and Iran (Zarch *et al.* 2015). The RDI is comparable to the FAO Aridity Index (Tsakiris *et al.* 2007).

Together, Figures 6 and 7 show that the SPI/SPEI and the RDI/Adjusted RDI all picked up the past extreme drought events that took place in 1976, 1989, 2005 and 2011. Drier than average events were also observed in 1963, 1964, 1984, 1989, 1996, 2003, and 2009. However, the severity of the drought events was slightly higher when using the *SPEI* index. It was also noticed that based on the *SPI/SPEI* drought index the total percentage of the wet years was higher than the total percentage of dry years.

Figure 8 shows the significant change in soil moisture indicators WI and SMD during the dry summer months of 1975 and 1976 and the recovery of soil moisture in 1977. During the dry summer months of 1976, the soil moisture deficit of the root zone reached 91 mm. The severity of the 1975 and 1976 drought events is indicated by the fact that the SMD did not drop back

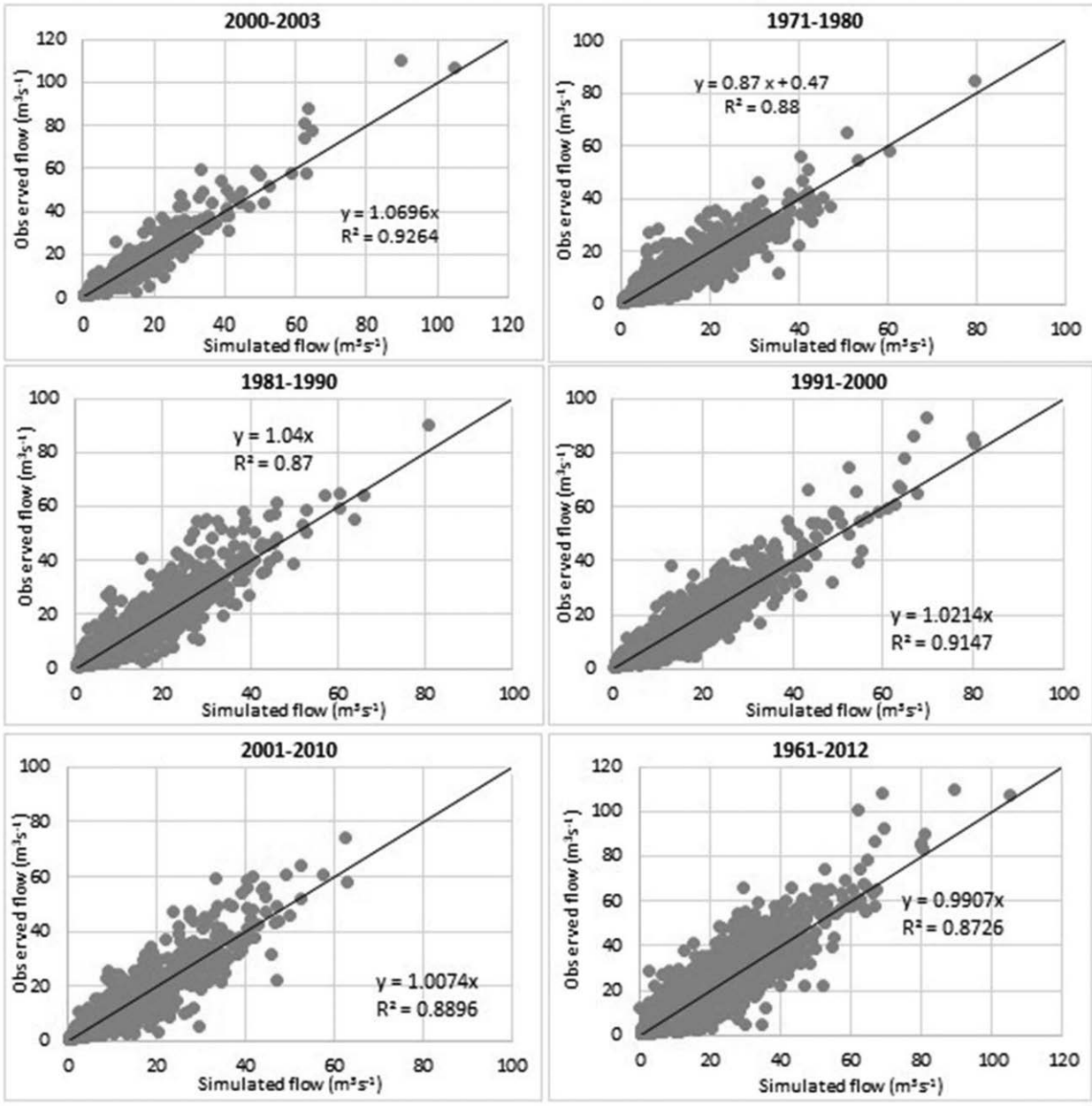

Figure 5 | Relationship between the observed and the simulated flow during the model calibration and model validation over a decadal time scale and over the entire period.

to zero due to the continuation of the dry conditions into the winter months. During the 1977 winter months, above average winter rainfall brought the SMD back to zero. The WI dropped below the winter value of 1.0, reaching values as low as 0.1 during the extreme drought of the summer of 1976 and thus mirrored the SMD trend.

Impact of future climate change on the water resources

Under all future emission scenarios of the UKCP09, using the joint probability seasonal change factors nine scenarios (three time periods and three emission scenarios) were applied. The change in temperature (in °C) and rainfall (in %), at the most likelihood (central estimate) probability

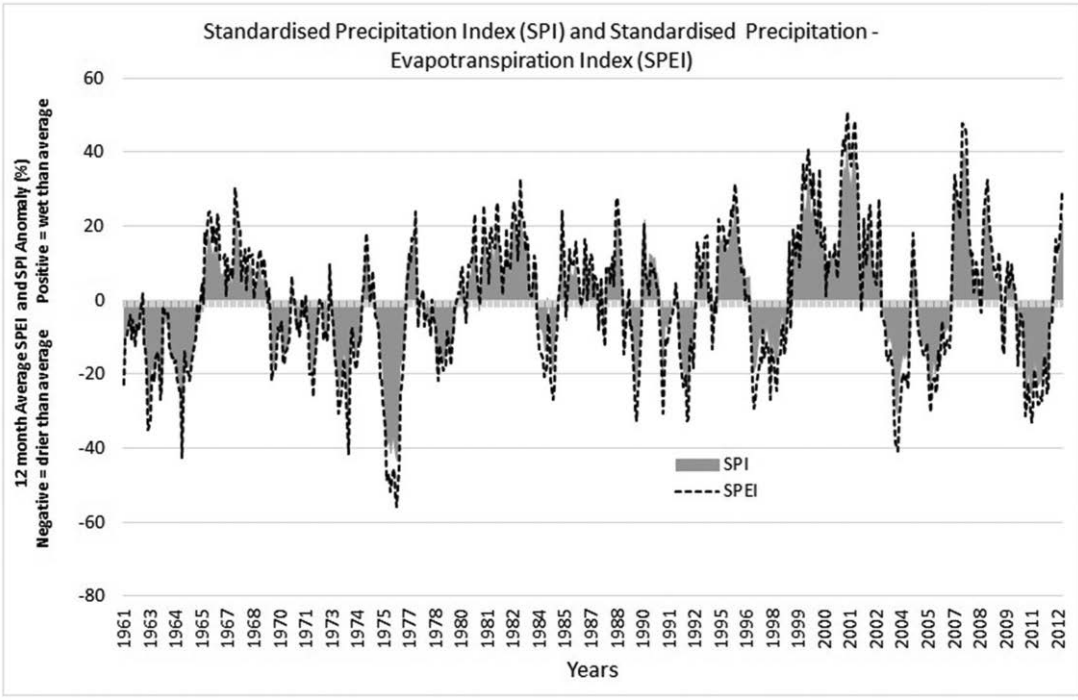

Figure 6 | The standardized precipitation index (SPI) and Standardized precipitation-evapotranspiration index (SPEI) of Ebbw catchment from 1961–2012.

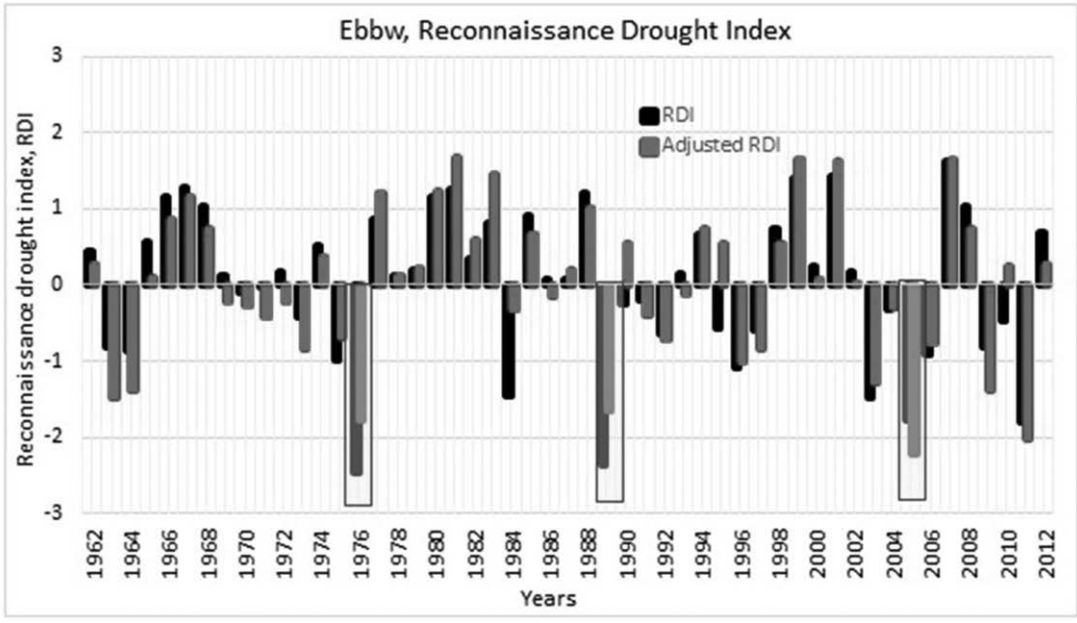

Figure 7 | Historic RDI (Reconnaissance drought index) based on potential evapotranspiration total rainfall and the adjusted RDI calculated using net-rainfall and actual evapotranspiration for the Ebbw catchment during the period 1962–2012. The severe drought events are highlighted in yellow.

level were input to the DiCaSM model and applied to the 1961–1990 baseline climate data (Table 1). The climate change projection of the UKCP09 by using the weather generator daily data of temperature, rainfall, vapour pressure and net radiation for 100 realizations of each 30-year period (900 realization files in total) were also

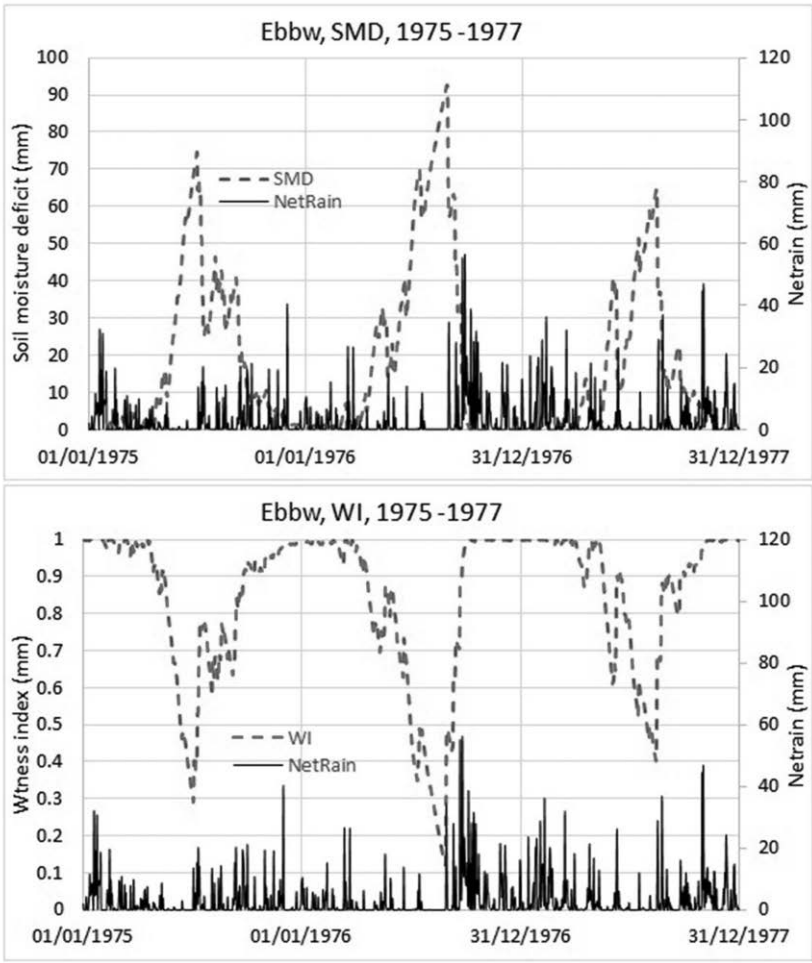

Figure 8 | Soil moisture deficit (SMD) and the Wetness Index (WI) at root-zone for the Ebbw catchment during the period 1975–1977.

employed in the DiCaSM model as a daily input of the three time periods and the three emission levels.

Impact on streamflow

The streamflow projections under both the simplified change factors (joint probability, JP) and the weather generator (WG) indicated that the streamflow is likely to increase in winter and to decrease in spring, summer and autumn, relative to the baseline period, under all emission scenarios (Figure 9). The seasonal variations are listed hereunder:

Impact on steamflow during winter (December, January, February, DJF). Using joint probability, the increase in streamflow during the 2020s is predicted to be approximately 4.5%, irrespective of the emission scenario. In the 2050s, a 5.7% increase in streamflow is expected under low emission, but under medium and high emission scenarios the increase would be approximately 13%. In the 2080s, the increase under low emissions would be 6.9%, while under medium and high emissions the increase would be approximately 18%.

Using the weather generator data, the increase in streamflow during the 2020s is predicted to be approximately 5% under low emission, 3.5% under medium and 4.8% under high emission scenario. In the 2050s, an increase of 6.2%, 7.3% and 8.5% is expected under low, medium and high emissions, respectively. In the 2080s, the increase would be 8.3%, 10.6% and 13.4% under low, medium and high emissions, respectively.

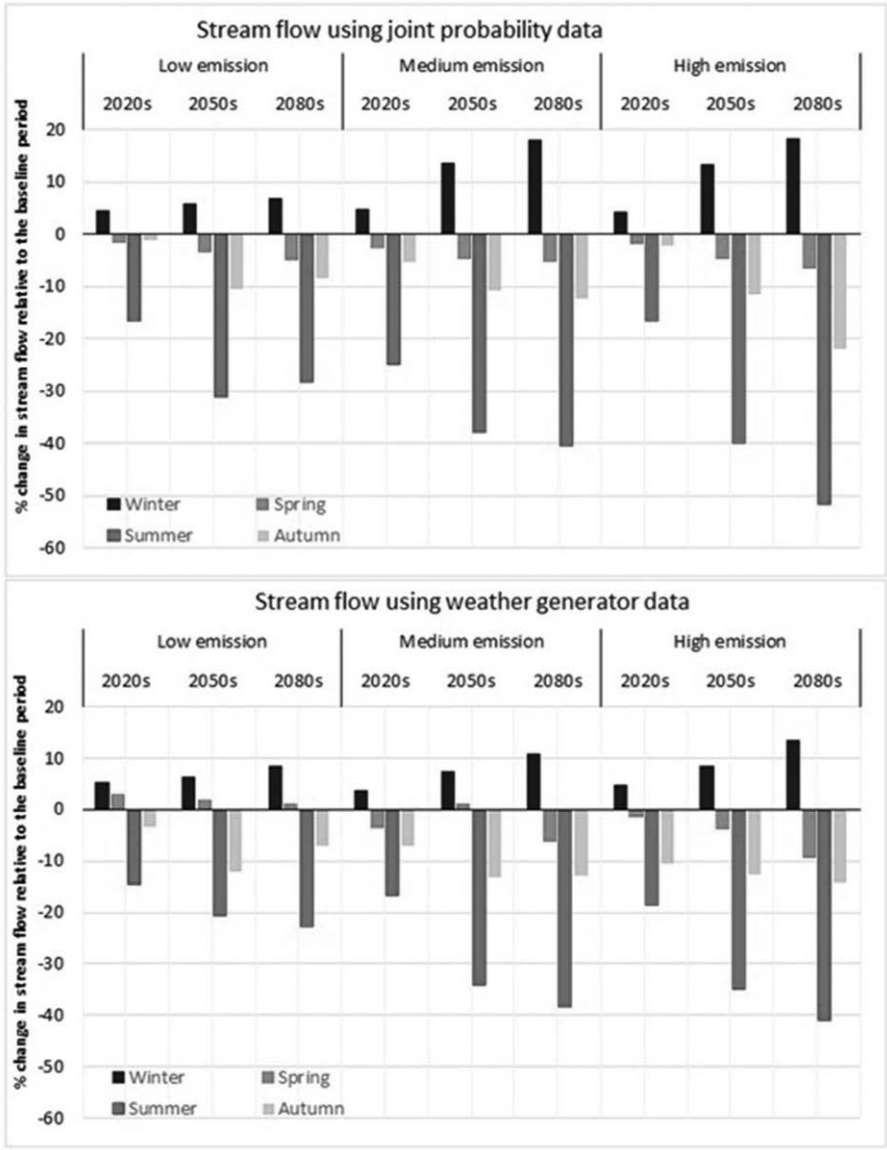

Figure 9 | Ebbw percentage change in streamflow based on joint probability projection (JP) and Weather Generator (WG) of UKCP09.

Impact on streamflow during spring (March, April, May, MAM). Using joint probability, the predicted decrease in streamflow during the 2020s would be −1.5% to −2.5%, with little impact of the emission scenario. During the 2050s, streamflow would decrease by −3.4% under low emission and by approximately −4.5% under medium and high emission scenarios. During the 2080s, the decrease would be approximately −5% under low and medium emissions and −6.6% under high emissions.

Using the weather generator data, streamflow during the 2020s is predicted to slightly increase by 2.8% under low emission and decrease by −3.5% under medium emissions and −1.5% under high emissions. During the 2050s, there is also a small increase by 1.7% and 1.1% under low and medium emission, respectively, but a decrease of −3.9% under high emission scenarios. During the 2080s there is, a tiny increase of 0.9% under low emission and a decrease by −6.0% and −9% under medium and high emission scenarios, respectively.

Impact on streamflow during summer (June, July, August, JJA). Using joint probability, the predicted decrease in streamflow during the 2020s would be approximately −16.5% under low and high emission scenarios and −25% under medium emission scenario. During the 2050s, streamflow would decrease by −31.2%, −37.9% and −39.9% under low, medium and high emissions, respectively. During the 2080s, the decrease would be approximately −28.2%, −40.5% and −51.8% under low, medium and high emissions, respectively.

Using the weather generator data, the decrease in streamflow during the 2020s is predicted to be approximately −14.5%, 16.8% and −18.4% under low, medium and high emissions, respectively. During the 2050s the decrease is predicted to be −20.5% under low emission and approximately −34% under medium and high emission scenarios. During the 2080s, the decrease is predicted to be −22.8%, −38.4% and −40.9% under low, medium and high emission scenarios, respectively.

Impact on streamflow during autumn (September, October, November, SON). Using joint probability, the predicted decrease in streamflow during the 2020s would be −1.2%, −5.6% and −2.1% under low, medium and high emission scenarios, respectively. During the 2050s, streamflow would decrease by −10.5% to −11.4%, with little effect of the emission level. During the 2080s, the decrease would be −8.3%, −12.3% and −22.0% under low, medium and high emissions, respectively. Using the weather generator data, the decrease in streamflow during the 2020s is predicted to decrease by −3.5%, −7.1% and −10.5% under low, medium and high emission, respectively. During the 2050s the decrease is predicted to be −12.1%, −13.2% and −12.5% under low, medium and high emission, respectively. During the 2080s, the decrease is predicted to be −7.1%, −12.9% and −14.3% under low, medium and high emission scenarios, respectively.

Impact on groundwater recharge

Projections are showing that, whether using joint probability or weather generator, groundwater recharge will increase during winter and decrease during summer, spring and autumn, relative to the baseline period, under all emission scenarios (Figure 10). The seasonal variations are listed hereunder

Impact on groundwater recharge during winter (DJF). Using joint probability, in the 2020s, an increase of 4.0%, 4.4% and 3.9% is projected under low, medium and high emissions, respectively. In the 2050s, the increase would be 5.0%, 13% and 12.7% under low, medium and high emission scenarios, respectively. In the 2080s, the increase would be 5.9%, 17% and 17.4% under low, medium and high emissions, respectively.

Using weather generator data, for the 2020s, the increase would be 3.9%, 2.8% and 2.1% under low, medium and high emissions, respectively. In the 2050s the increase is projected to be approximately 10.3%, 10.6% and 12.4% under low, medium and high emissions, respectively. In the 2080s the increase would be 10.7%, 14.7% and 14.5% under low, medium and high emissions, respectively.

Impact on groundwater recharge during spring (MAM). Using joint probability, a decrease of −4.5%, −5.5% and −4.4% is projected for the 2020s under low, medium and high emissions, respectively. In the 2050s, the decrease would be −7.4%, −10.2% and −10.4% under low, medium and high emissions, respectively. In the 2080s, the decrease would be −10.3%, −12.3% and −15.4% under low, medium and high emissions, respectively.

Using the weather generator data, for the 2020s, there would be a small increase of 1.1% under low emission scenario but a decrease of −6.0% and −5.8% under medium and high emissions, respectively, were projected. In the 2050s the projected changes are approximately −10%, +0.3% and −2.4% under low, medium and high emissions, respectively and in the 2080s the decrease is projected to be approximately −6%, −1.35% and −4.5% under low, medium and high emissions, respectively.

Impact on groundwater recharge during summer (JJA). Using joint probability, a decrease of −29.5%, −42.6% and −29.7% is projected for the 2020s under low, medium and high emissions scenarios, respectively. During the 2050s the decrease would be −52.7%, −63.4% and −66.7%% under low, medium and high emissions, respectively and by the 2080s, the decrease would be −47.6%, −68.5%

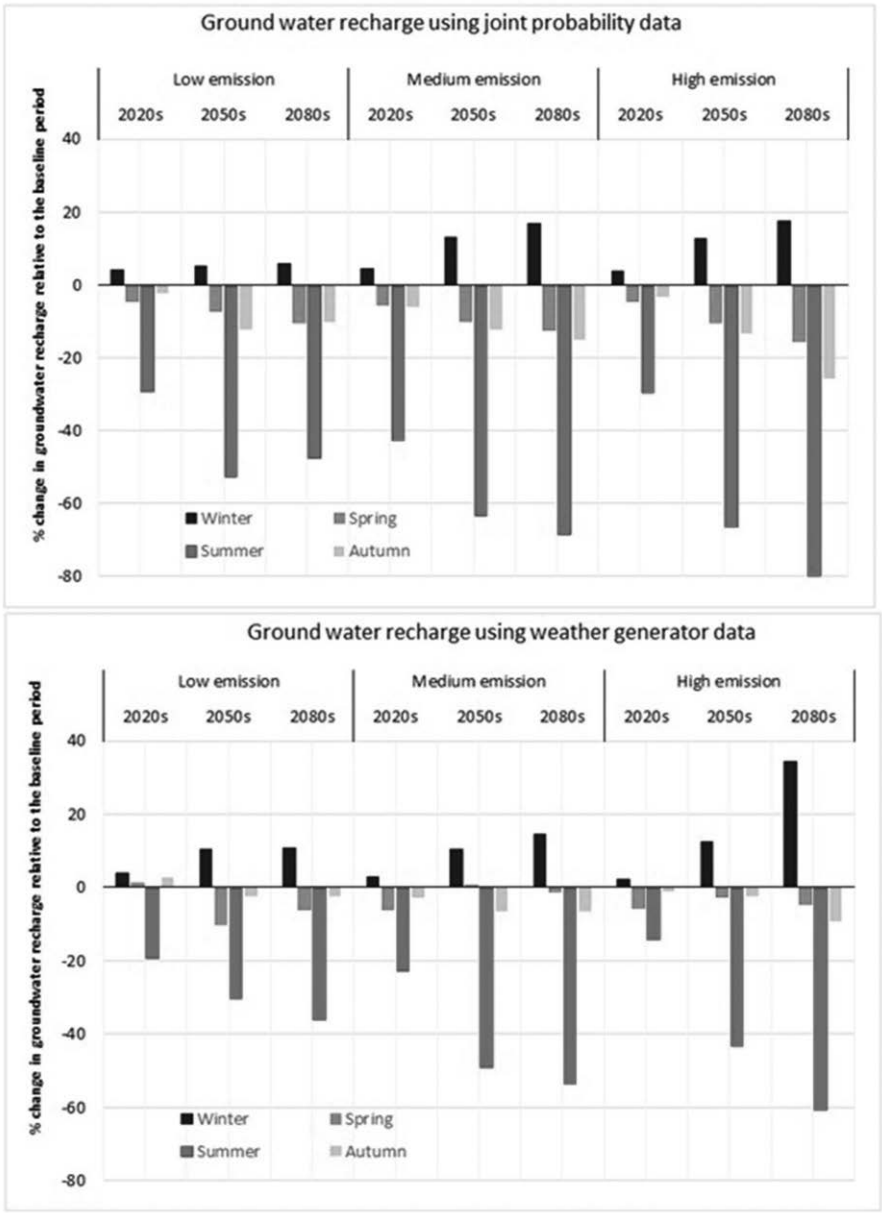

Figure 10 | Ebbw percentage change in groundwater recharge based on joint probability projection (JP) and Weather Generator (WG) of UKCP09.

and −83.9% under low, medium and high emissions, respectively.

Using weather generator data the decrease during the 2020s would be −19.3%, −22.6% and −14.2% under low, medium and high emission scenarios, respectively; −30.4%, −49.1% and −43.2% for low, medium and high emission during the 2050s, respectively and −36.2%, −53.6% and −60.6% for low, medium and high emissions during the 2080s, respectively.

Impact on groundwater recharge during autumn (SON). Using joint probability, a decrease of −2.2%, −5.9% and −3.4% is projected for the 2020s under low, medium and high emissions scenarios, respectively. During the

2050s the decrease would be −12.2%, −12.4% and −13.3%, under low, medium and high emissions, respectively and by the 2080s, the decrease would be −10.4%, −14.9% and −25.8% under low, medium and high emissions, respectively.

Using weather generator data during the 2020s there would be a small increase of 2.8% under low emission, and a decrease of −2.7% to −1.1% under medium and high emission scenarios, respectively. During the 2050s the decrease would be −2.3%, −6.4% and −2.5% for low, medium and high emissions, respectively; and −2.4%, −6.4% and −9.3% for low, medium and high emissions, respectively, during the 2080s.

Drought indices under climate change scenarios

Future seasonal changes in the RDI, SMD, WI drought indicators in addition to actual evapotranspiration, AE, were predicted using joint probability.

Future SMD, WI and evapotranspiration

The analysis (Figure 11) suggested a possible increase in soil moisture deficit, *SMD*, an increase in both potential and actual evapotranspiration and a decrease in wetness index of root-zone, under the three emission scenarios and for the three selected time periods. The changes increased with increasing the emission level and with time. The 2020s had the smallest changes while the 2080s had the largest changes. The highest projected increase/decrease was associated with the high emission scenarios of the 2080s where soil moisture deficit, wetness index, potential and actual evapotranspiration were changed by 145.3%, −20%, 130% and 106%, respectively.

Future annual and seasonal Reconnaissance Drought Index (RDI)

The projected number and severity of drought events is viewed in relation to the historic 1961–1990 baseline

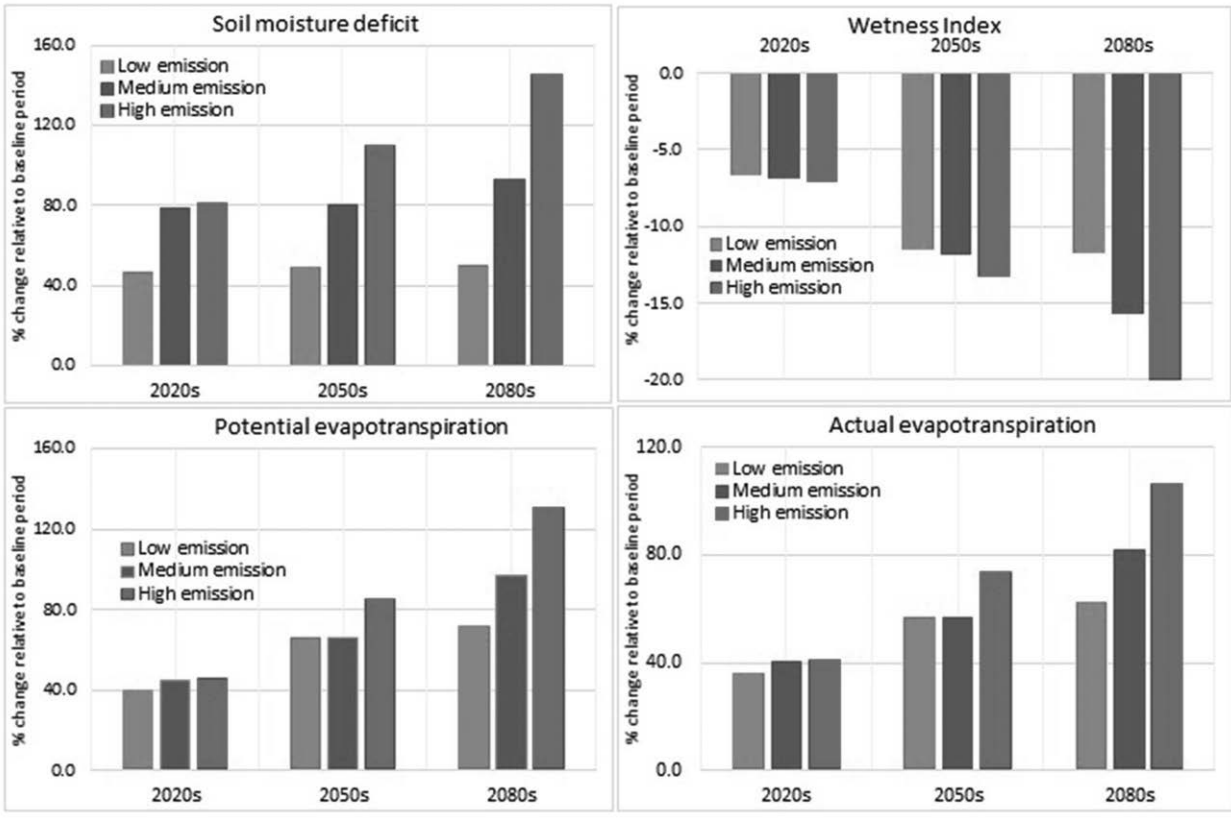

Figure 11 | Changes in soil moisture deficit, actual and potential evapotranspiration and the wetness index at root zone under all emission scenarios based on UKCP09 joint probability.

period, seasonal and annual changes are given in Table 3. During the 2020s the number and severity of the drought events is expected to be similar to the baseline period. Figure 12 shows the changes on an annual basis. The number of possible future drought events based on RDI calculation using JP and WG data are very close. Under low emission, the number of drought events during the 2020s looks similar to the baseline number of drought events, while the 2050s and 2080s show a possible increase by one severe drought event while under medium emission, only the 2080s showed a possible increase by one moderate and one severe drought event. High level emission showed a possible increase in the 2050s and 2080s in the number of severe and extreme drought events.

The annual results commonly integrate the seasonal variation (Table 3). The table shows that in winter, the total number of drought events for the three periods together (2020 to 2099) is likely to be 15, 19 and 21 while the number for spring is 13, 16 and 16 for low, medium and high emissions, respectively. For summer, the number of drought events is expected to be 17, 18 and 20 and for autumn, 15, 16, and 16 for low, medium and high emissions, respectively. Given the baseline data of 30 years (1961–1990) where the number of drought events was 5, 3, 5, and 4 for winter, spring, summer and autumn, respectively, the projection indicates a possible significant increase in the drought events from the 2020s to the 2080s.

Impact of future land use changes on some hydrological variables

Based on the existing land use practices, shown in Figure 2, five possible land use scenarios were considered (Table 4). In the first scenario, all crops and grass areas were replaced by broadleaf woodland. This resulted in a decrease in streamflow by −2.2% in winter, −6.3% in spring, −8.8% in summer and –3.9% in autumn, and a decrease in groundwater recharge of 4.8% in winter, −8.1% in spring, −12.9% in summer and −6.1% in autumn. The second land-use scenario was to replace the heather area by coniferous woodland, which resulted in a tiny decrease of $\leq -1\%$ in streamflow and groundwater recharge in all seasons. The third scenario was to replace the grass area by coniferous woodland. The analysis revealed a small decrease with maximum values of $\leq -5\%$, in streamflow and $\leq -7\%$ in groundwater recharge. The fourth land use scenario was to expand urban area by replacing 25% of the total grass area. This change led to a slight maximum increase in streamflow of $\leq 5\%$, and a maximum decrease in groundwater recharge of $\leq -10\%$. In the fifth scenario, the grass

Table 3 | Severity of the drought events observed using the Reconnaissance Drought Index (RDI) during the annual and seasonal time scales under all emission scenarios

Time period	Annual drought severity			Winter			Spring			Summer			Autumn		
	Extreme	Severe	Moderate	Extreme	Severe	Moderate	Extreme	Severe	Moderate	Extreme	Severe	Moderate	Extreme	Severe	Moderate
1961-1990	1	3	1	1	1	3	2	0	1	0	4	1	0	3	1
Low 2020s	1	3	1	1	1	3	2	1	1	0	4	1	0	3	2
Low 2050s	1	4	1	1	1	3	2	1	1	0	4	1	1	2	2
Low 2080s	1	4	1	1	2	2	1	3	1	1	4	2	0	4	1
Med. 2020s	1	3	1	1	1	3	2	1	1	1	3	1	0	3	2
Med. 2050s	2	3	1	1	2	4	3	2	1	1	3	3	1	2	2
Med. 2080s	2	3	2	1	2	4	3	1	2	2	3	1	1	2	3
High 2020s	1	3	1	1	1	3	2	1	1	1	3	1	0	3	2
High 2050s	2	3	2	1	2	4	3	1	1	1	4	2	1	2	2
High 2080s	3	2	2	2	2	5	3	2	2	2	4	2	1	3	2

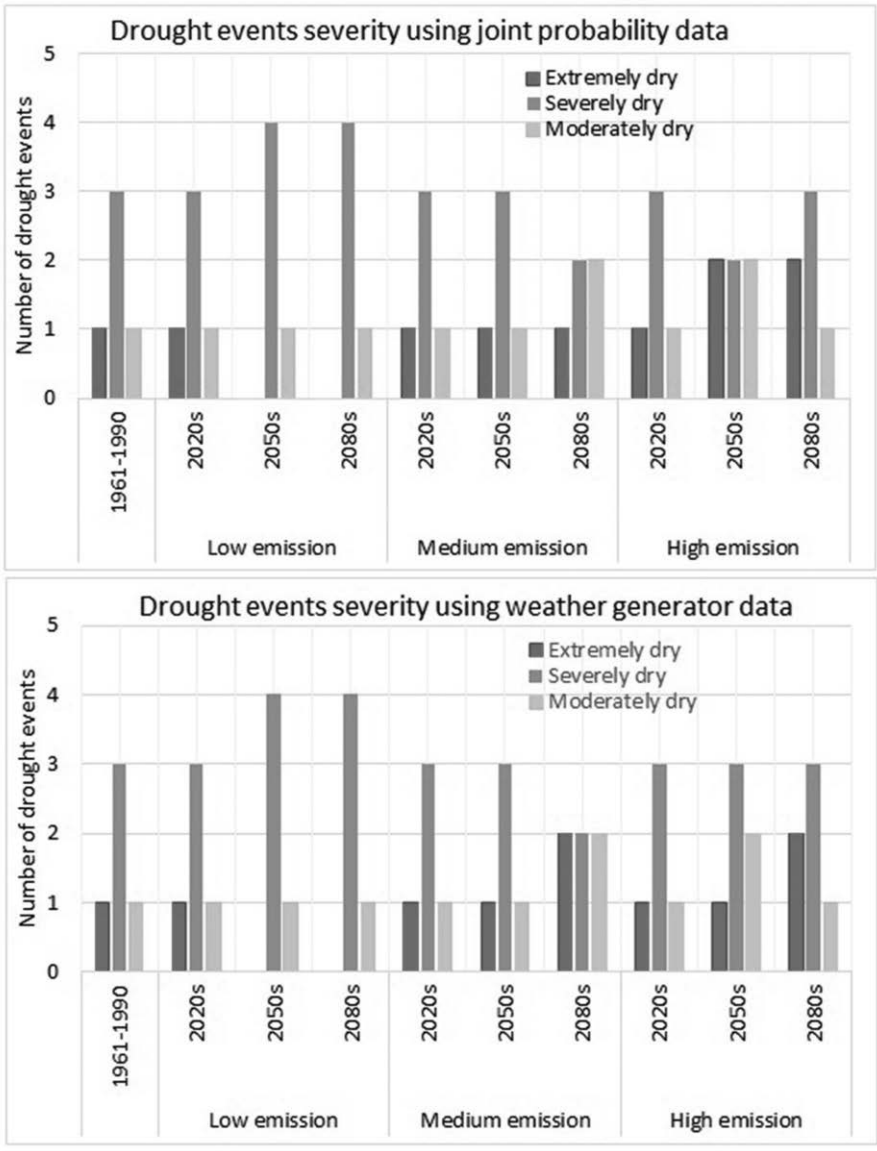

Figure 12 | Severity of the drought events observed using the Reconnaissance Drought using the Reconnaissance drought index, RDI calculated using the joint probability (top) and weather generator (bottom) data.

area was replaced by barley, which is generally considered as the drought resistant crop. Replacing the grass area with barley crop showed a slight increase, with maximum values of $\leq$4.4% in the streamflow and $\leq$5.1% in groundwater recharge. The reduction in streamflow and groundwater recharge are due to the increase in actual evapotranspiration and subsequently the increase in soil moisture deficit caused by reduced rainfall and increased temperature. When comparing the impacts of land use changes to the climate change, the impact of climate change is more significant than the land use changes.

DISCUSSION

The future climate change impact indicated that the streamflow and groundwater recharge when using the simplified change factors (joint probability, JP) and the weather

Table 4 | Percent changes in streamflow and groundwater recharge due to land use changes

		Change in land-use type				
Hydrological variables	**Seasons**	**All crops and grass replaced by Broadleaf trees**	**Heather replaced by Coniferous trees**	**Grass replaced by Coniferous trees**	**25% of grass area replaced by Urban**	**Grass Replaced by Barley**
River flow	Winter	−2.22	−0.73	−2.28	1.32	3.05
	Spring	−6.29	−0.41	−3.25	2.59	2.32
	Summer	−8.78	−0.02	−4.59	4.47	0.08
	Autumn	−3.91	−0.58	−3.00	2.57	4.41
Groundwater recharge	Winter	−4.78	−0.97	−2.45	−2.05	3.39
	Spring	−8.08	−0.26	−4.21	−5.11	2.64
	Summer	−12.86	0.62	−6.88	−10.36	1.15
	Autumn	−6.11	−0.88	−3.15	−3.71	5.11

generator (WG) are likely to increase in winter and to decrease in spring, summer and autumn, relative to the baseline period, under all emission scenarios. The streamflow in wintertime is expected to increase by up to 18% and 13% when using JP and WG data, respectively. At the same time, the winter groundwater recharge is also expected to increase when using JP and WG data by up to 17% and 14%, respectively. The increase gets bigger with time and with increasing the emission level, being the highest by the 2080s under high level emission scenario.

The increase in winter precipitation was associated with high water losses by evaporation due to the increased temperature. This has resulted in a lower than expected increase in streamflow and groundwater recharge. This result is of importance for the Ebbw catchment as there are a number of reservoirs within the catchment boundary, i.e. at the north of the Ebbw catchment the Shon Sheffrey's reservoir which intercepts about 300 mega-litres run off water per day, further down, the Lanton Loch which intercepts 20 mega-litres per day and a few small reservoirs that intercept up to 6 mega-litres water per day. These reservoirs supply water to users within the catchment during winter and spring.

In spring, the predicted decrease in streamflow when using JP and WG data was up to −7% and up to −9% while the recharge is projected to decrease by up to −15% and −5%, respectively. This small decrease in streamflow and groundwater recharge is possibly due to the fact that during the spring season, the evaporation is relatively low, and the soil is sufficiently wet except during the latter part of spring. The maximum decrease is associated with the high emission scenario and the 2080s period.

In summer, the predicted decrease in streamflow is significantly higher than in spring and can reach −52% and −41% when using JP and WG data, respectively. Using JP and WG data, the recharge is also likely to decrease significantly by −84% and −61%, respectively. A significant change in groundwater recharge during the summer months is due to the enhanced evapotranspiration together with the decreased precipitation which results in high soil moisture deficit and subsequently large reduction in streamflow and groundwater recharge. The maximum decrease is associated with the high emission scenario and the 2080s period.

The severity of the reduction in streamflow and groundwater recharge, particularly during summer, could lead to critical water shortage for the domestic, industrial and agricultural water supplies. The latter is more significant as river water abstraction is very significant during the summer months as the storage reservoirs dry up during the summer. The combined effect of decreasing rainfall with the increasing temperature (JP) with an increase in net-radiation (WG) could result in higher evapotranspiration during the summer season leading to reduced flow, particularly under high emission scenarios when the temperature is likely to increase by 4.6 ^{0}C and rainfall is likely to decrease by up to 34% by the end of the century (Table 1).

In autumn, the decrease in streamflow can reach −22% and −14% when using JP and WG data, respectively.

Meanwhile, the groundwater recharge using JP and WG data is likely to decrease by −26% and −9%, respectively. As seen in Table 1, with reductions in precipitation in autumn and spring (enhanced by higher evaporation) soil saturation conditions will occur less frequently, and precipitation events will be less likely to generate high flows.

A decrease in precipitation and increase in temperature resulted in higher evapotranspiration during the summer months, leading to higher soil moisture deficit which was carried over to the autumn months. Although no significant change in precipitation occurred during the autumn season, the drier soil conditions and increasing temperature resulted in a significant increase in *SMD* in the autumn season. In addition to rainfall and temperature, evapotranspiration was a key factor in causing high soil moisture deficit.

Higher evapotranspiration combined with lower rainfall during the summer months would result in an increase in soil moisture deficit and subsequently low groundwater recharge in autumn months under all emission scenarios. However, the level of the decrease is much higher in the second half of the century (2050s & 2080s) under high emission scenarios. Findings of the study suggest that climate change could significantly affect the groundwater recharge in Ebbw catchment with significant variations between seasons.

The biggest change in the actual evapotranspiration and soil moisture deficit was observed under high emission scenarios due to the increasing temperature which significantly affects both the surface and groundwater resource availability. This increase in actual evapotranspiration and soil moisture deficit resulted in a decrease of wetness index, Figure 11.

The drought indices used in this study clearly identified all the historic droughts events, i.e. the 1970s, 1980s, 1990s, as reported by Marsh and Monkhouse (1993). The standardized precipitation index, *SPI* indicated the significantly negative deviation from the average precipitation in the 1970s. This identification of the 1970s drought events has also been confirmed by the other drought indices like the reconnaissance drought index, *RDI*, soil moisture deficit, *SMD* and the wetness index, *WI* of the root-zone (as shown for the period 1975–1977 in Figure 8).

Application of a wider range of drought indices could be used to identify different types of drought. For example, in agriculture, when soil moisture deficit, *SMD* or Wetness Index, *WI* of the root zone, reach a critical level, crops will need irrigation particularly during the summer months. This will require reliable water supplies to secure adequate yield. The *WI* value, if close to 1, would indicate a wet catchment with a possible runoff generation during the next rainfall event, therefore, it is a help to reservoir managers to know the *WI* in real time. The possible occurrence of drought events and their severity levels calculated by *RDI* would be helpful for short- and long-term planning by water authorities and water companies. Therefore, the findings from the modelling work can be used to review the future surface water abstraction regulations to be in line with the water resources availability as predicted by the hydrological models.

The DiCASM model proved to be a good tool to predict river flow and recharge to groundwater and is capable of simulating the effects of climate change on the different elements of the hydrological cycle. The future climate change scenarios suggested a decrease in groundwater recharge by 80% by the end of the century during the summer season. Also, the streamflow is likely to decrease by 50% during the summer months. The effect of low rainfall and high temperature was also expressed by the *RDI* drought index that was able to show frequency and the severity of the drought events, more importantly in the second half of the century (2050s & 2080s).

Considering the possibility of such droughts in the future, the agriculture and irrigation practices need to be adapted for the future as reduced water supply could be problematic for irrigation in summer. This has been reported in other studies (Weatherhead and Howden 2009; Knox *et al.* 2010), and considering the possible future increase in water demand for agriculture, a possible solution would be to consider less water-consuming crops. The implication of water abstractions during drought and low flow periods would reduce river flows possibly below the minimum environmental flow. Alternatively, restrictions on abstraction to maintain the minimum environmental flows may restrict crop yields and food, or energy production.

The impact of land use changes on streamflow and groundwater recharge was less than the impact of climate change. The change in land use from grass to barley or to urban did not show a big impact. However, a big impact

was produced when the grass and crops were replaced by trees. Trees have deeper roots and large canopies resulting in more rainfall interception; leading to lower net rainfall available for runoff and infiltration, large and deep roots resulting in more water uptake and transpiration; leading to larger soil moisture deficit and less recharge.

Previous studies using the DiCaSM model also quantified the impact of climate and land use changes on semiarid catchments. D'Agostino *et al.* (2010) studied the climate change scenarios for southern Italy, i.e. reduced winter rainfall by 5–10%, reduced summer rainfall by 15–20%, winter temperature rise by 1.25–1.5 °C and summer temperature rise by 1.5–1.75 °C. The results indicated that by 2050, groundwater recharge in the Candelaro catchment would decrease by 21–31% and streamflows by 16–23%. The model results also showed that the projected durum wheat yield up to 2050 is likely to decrease between 2.2% and 10.4% due to the future reduction in rainfall and increase in temperature. Montenegro and Ragab (2010) reported that the DiCaSM model forecasted a reduction of 35%, 68%, and 77%, in groundwater recharge, and by 34%, 65%, and 72%, in streamflow, for the time spans 2010–2039, 2040–2069, and 2070–2099, respectively, could take place for a dry future climate scenario. Introducing castor beans to the catchment would increase the groundwater recharge and streamflow, mainly if the caatinga areas would be converted into castor beans production. Changing an area of 1000 ha from caatinga to castor beans would increase the groundwater recharge by 46% and streamflow by 3%. If the same area of pasture is converted into castor beans, there would be an increase in groundwater recharge and streamflow of 24% and 5%, respectively. Such results are expected to contribute towards environmental policies for north-east Brazil and to biofuel production perspectives in the region. Montenegro and Ragab (2012) on another catchment in the semiarid north-east of Brazil reported the possibility of reduction in surface water availability by 13.90%, 22.63% and 32.91% in groundwater recharge and by 4.98%, 14.28% and 20.58% in surface flows for the time spans 2010–2039, 2040–2069, 2070–2099, respectively. This would cause severe impacts on water supply in the region. Changing land use from vegetables to sugar cane would result in decreasing groundwater recharge by almost 11%, and increasing streamflow by almost 5%. The combination of possible impacts of climate change and land use requires a proper plan for water resources management and mitigation strategies. In a study on two Cyprus catchments, Ragab *et al.* (2010) showed that by 2050, groundwater and surface water supplies would decrease by 35% and 24% for Kouris and 20% and 17% for Akrotiri, respectively. The gap between water supply and demand showed a linear increase with time. The results suggest that the DiCaSM model could be used as an effective tool for water authorities and decision makers to help balance demand and supply on the island.

CONCLUSIONS

The impact of climate change on Ebbw catchment's water resources using 52 years of data was carried out using the DiCaSM hydrological model. Following successful calibration and validation using the measured streamflow, the model was run with the climate change scenarios of UKCP09 for three periods (30 years each) up to 2099 under three emission scenarios: low, medium and high.

Drought indicators such as the reconnaissance drought index, RDI, the adjusted reconnaissance drought index, adjusted RDI, the standardized precipitation index, *SPI,* soil moisture deficit, *SMD* of the root zone and the wetness Index, *WI* of the root-zone, were able to reproduce the past drought events.

The data of future climate change were obtained from two sources of the UKCP09, simple change factors to temperature (± °C) and rainfall (%) using joint probability plot, JP and daily values of weather data generated by the weather generator, WG. Both JP and WG scenarios were implemented as inputs to the model. The projections indicated that the streamflow and groundwater recharge are likely to increase in winter and to decrease in spring, summer and autumn, relative to the baseline period, under all emission scenarios with the greatest decrease in groundwater recharge and the streamflow projected in the second half of the current century (2050s & 2080s) under high emission scenarios due to the projected drier summers with low rainfall and high temperatures.

Although the climate models projected an increasing trend in winter precipitation, this increase was not equally

converted into an increase in annual groundwater recharge and streamflow due to the relatively high losses by evapotranspiration. The analysis also revealed that the medium and high emission scenarios, severity and the frequency of future drought events are likely to increase with time and emission level as indicated by the drought indicators, adjusted Reconnaissance Drought Index, Soil Moisture Deficit and the Wetness Index of the root-zone.

The climate model suggested an increase in precipitation during the winter months. However, the increased flows into the reservoirs may not result in increased storage if the reservoirs are already full. This is very important for the Ebbw catchment where the reservoirs are usually full during the winter. The analysis of land use changes revealed that changing grass and arable areas to woodland would have a significant impact on water resources. Other land use changes such as replacing grass area with barley would not significantly affect the water resources. These research findings would help in planning for perhaps extra water infrastructure work if needed, such as building more reservoirs or water transfer pipelines from water-rich to water-poor regions and planning for irrigation water demand under different climatic conditions.

ACKNOWLEDGEMENT

The authors acknowledge the NERC funding for this 4-year 'Drought Risk and You, DRY' project, grant reference NE/L010292/1. We are also very thankful to our CEH colleagues especially Yan Weigang, Egon Dumont, Virginie Keller and James Blake who helped in preparing the model input data. The authors are also very thankful to Prof. Lindsey McEwen and Ms Liz Roberts, UWE, who helped in organising Local Advisory Group meetings for the Ebbw catchment. The authors would like to acknowledge the data sources: background mapping from Ordnance Survey ('1:250 000 Scale Colour Raster'). Catchment boundary and gauging station location data from Centre for Ecology and Hydrology (Morris *et al.* 1990; Morris and Flavin 1994). River and waterbody data from Centre for Ecology and Hydrology ('Digital Rivers 50 km GB' Web Map Service). Land cover data from Centre for Ecology and Hydrology (Land Cover Map 2007 (25 m raster, GB) Web Map Service (Morton *et al.* 2011). Standardized Precipitation Index time series for IHU groups (1961–2012) [SPI_IHU_groups] data licensed from NERC Centre for Ecology & Hydrology. Soils data courtesy of Cranfield University (1:250 000 Soilscapes for England and Wales Web Map Service). Hydrogeology data from British Geological Survey (DiGMapGB 1:625 000 scale digital hydrogeological data).

REFERENCES

Alexander, L. V., Tett, S. F. & Jonsson, T. 2005 Recent observed changes in severe storms over the United Kingdom and Iceland. *Geophysical Research Letters* **32**, L13704.

AL-Faraj, F. A., Scholz, M., Tigkas, D. & Boni, M. 2015 Drought indices supporting drought management in transboundary watersheds subject to climate alterations. *Water Policy* **17**, 865–886.

Allen, R. G., Pereira, L. S., Raes, D. & Smith, M. 1998 *Crop evapotranspiration-Guidelines for computing crop water requirements-FAO Irrigation and drainage paper 56*, Vol. 300. FAO, Rome, p. D05109.

Arnell, N. W. 2011 Incorporating climate change into water resources planning in England and Wales. *JAWRA Journal of the American Water Resources Association* **47**, 541–549.

Bachmair, S., Tanguy, M., Hannaford, J. & Stahl, K. 2018 How well do meteorological indicators represent agricultural and forest drought across Europe? *Environmental Research Letters* **13**, 034042.

Barker, L. J., Hannaford, J., Parry, S., Smith, K. A., Tanguay, M. & Prudhomme, C. 2019 Historic hydrological droughts 1891–2015: systematic characterisation for a diverse set of catchments across the UK. *Hydrology and Earth System Sciences* **23** (11), 4583–4602. https://doi.org/10.5194/hess-23-4583-2019.

Bastola, S., Murphy, C. & Fealy, R. 2012 Generating probabilistic estimates of hydrological response for Irish catchments using a weather generator and probabilistic climate change scenarios. *Hydrological processes* **26**, 2307–2321.

Bento, V. A., Gouveia, C. M., Dacamara, C. C. & Trigo, I. F. 2018 A climatological assessment of drought impact on vegetation health index. *Agricultural and Forest Meteorology* **259**, 286–295.

Byakatonda, J., Parida, B., Moalafhi, D. & Kenabatho, P. K. 2018 Analysis of long term drought severity characteristics and trends across semiarid Botswana using two drought indices. *Atmospheric Research* **213**, 492–508.

Ceh 2014. *CEH digital river network of Great Britain web map service*. Available from: https://data.gov.uk/dataset/

3c7ea82e-83e0-45a3-9a3f-8ba653b3211b/ceh-digital-river-network-of-great-britain-web-map-service (Accessed 2014).

Cloke, H., Jeffers, C., Wetterhall, F., Byrne, T., Lowe, J. & Pappenberger, F. 2010 Climate impacts on river flow: projections for the Medway catchment, UK, with UKCP09 and CATCHMOD. *Hydrological Processes* **24**, 3476–3489.

D'agostino, D. R., Trisorio, L. G., Lamaddalena, N. & Ragab, R. 2010 Assessing the results of scenarios of climate and land use changes on the hydrology of an Italian catchment: modelling study. *Hydrological processes* **24**, 2693–2704.

Grover, V. I. 2015 Impact of climate change on the water cycle. In: *Managing Water Resources under Climate Uncertainty* (S. Shrestha, A. K. Anal, P. A. Salam & M. van der Valk, eds). Springer Cham, Switzerland.

Gudmundsson, L., Bremnes, J., Haugen, J. & Engen-Skaugen, T. 2012 Downscaling RCM precipitation to the station scale using statistical transformations-a comparison of methods. *Hydrology and Earth System Sciences* **16**, 3383.

Gupta, H. V., Kling, H., Yilmaz, K. K. & Martinez, G. F. 2009 Decomposition of the mean squared error and NSE performance criteria: Implications for improving hydrological modelling. *Journal of Hydrology* **377**, 80–91.

Harris, C., Quinn, A. & Bridgeman, J. 2014 The use of probabilistic weather generator information for climate change adaptation in the UK water sector. *Meteorological Applications* **21**, 129–140.

Hartick, C., Furusho, C., Goergen, K. & Kollet, S. 2019 *Interannual, probabilistic prediction of water resources over Europe following the heatwave and drought 2018*. Preprint at, https://eartharxiv.org/h43xz/.

Karavitis, C. A., Tsesmelis, D. E., Skondras, N. A., Stamatakos, D., Alexandris, S., Fassouli, V., Vasilakou, C. G., Oikonomou, P. D., Gregorič, G. & Grigg, N. S. 2014 Linking drought characteristics to impacts on a spatial and temporal scale. *Water Policy* **16**, 1172–1197.

Kendon, M., Marsh, T. & Parry, S. 2013 The 2010–2012 drought in England and Wales. *Weather* **68**, 88–95.

Knox, J., Morris, J. & Hess, T. 2010 Identifying future risks to UK agricultural crop production: Putting climate change in context. *Outlook on Agriculture* **39**, 249–256.

Kunz, J., Löffler, G. & Bauhus, J. 2018 Minor European broadleaved tree species are more drought-tolerant than Fagus sylvatica but not more tolerant than Quercus petraea. *Forest Ecology and Management* **414**, 15–27.

Ledbetter, R., Prudhomme, C. & Arnell, N. 2012 A method for incorporating climate variability in climate change impact assessments: Sensitivity of river flows in the Eden catchment to precipitation scenarios. *Climatic Change* **113**, 803–823.

Livada, I. & Assimakopoulos, V. 2007 Spatial and temporal analysis of drought in Greece using the Standardized Precipitation Index (SPI). *Theoretical and applied climatology* **89**, 143–153.

Marsh, T. 1996 The 1995 UK drought-a signal of climatic instability? Technical note. *Proceedings of the Institution of Civil Engineers-Water Maritime and Energy* **118**, 189–195.

Marsh, T. & Monkhouse, R. 1993 Drought in the United Kingdom, 1988–92. *Weather* **48**, 15–22.

Marsh, T., Cole, G. & Wilby, R. 2007 Major droughts in England and Wales, 1800–2006. *Weather* **62**, 87–93.

Mckee, T. B., Doesken, N. J. & Kleist, J. 1993 The relationship of drought frequency and duration to time scales. In *Proceedings of the 8th Conference on Applied Climatology*. American Meteorological Society, Boston, MA, pp. 179–183.

Michaelides, S. & Pashiardis, S. 2008 Monitoring drought in Cyprus during the 2007–2008 hydrometeorological year by using the standardized precipitation index (SPI). *European Water* **23**, 123–131.

Montenegro, A. & Ragab, R. 2010 Hydrological response of a Brazilian semi-arid catchment to different land use and climate change scenarios: a modelling study. *Hydrological Processes*. **24** (19), 2705–2723.

Montenegro, S. & Ragab, R. 2012 Impact of possible climate and land use changes in the semi-arid regions: a case study from North Eastern Brazil. *Journal of Hydrology* **434–435**, 55–68.

Morris, D. & Flavin, R. 1994 *Sub-set of the UK 50 m by 50 m hydrological digital terrain model grids*. NERC, Institute of Hydrology, Wallingford.

Morris, D., Flavin, R. & Moore, R. 1990 A digital terrain model for hydrology. In: *4th International Symposium on Spatial Data Handling*, 23–27 July 1990, Zürich, pp. 250–262.

Morton, D., Rowland, C., Wood, C., Meek, L., Marston, C., Smith, G., Wadsworth, R. & Simpson, I. 2011 *Final Report for LCM2007-the new UK land cover map*. Countryside Survey Technical Report No 11/07.

Nash, J. E. & Sutcliffe, J. V. 1970 River flow forecasting through conceptual models part I–A discussion of principles. *Journal of hydrology* **10**, 282–290.

NRFA 2014. *National River flow Archive*. Available from: http://nrfa.ceh.ac.uk/ (Accessed 2014).

Parsons, D. J., Rey, D., Tanguy, M. & Holman, I. P. 2019 Regional variations in the link between drought indices and reported agricultural impacts of drought. *Agricultural Systems* **173**, 119–129.

Phillips, I. D. & Mcgregor, G. R. 1998 The utility of a drought index for assessing the drought hazard in Devon and Cornwall, South West England. *Meteorological Applications* **5**, 359–372.

Ragab, R. & Bromley, J. 2010 IHMS–Integrated Hydrological Modelling System. Part 1. Hydrological processes and general structure. *Hydrological processes* **24**, 2663–2680.

Ragab, R., Bromley, J., Dörflinger, G. & Katsikides, S. 2010 IHMS–Integrated Hydrological Modelling System. Part 2. Application of linked unsaturated, DiCaSM and saturated zone, MODFLOW models on Kouris and Akrotiri catchments in Cyprus. *Hydrological processes* **24**, 2681–2692.

Rio, M., Rey, D., Prudhomme, C. & Holman, I. P. 2018 Evaluation of changing surface water abstraction reliability for supplemental irrigation under climate change. *Agricultural Water Management* **206**, 200–208.

Robinson, E., Blyth, E., Clark, D., Comyn-Platt, E., Finch, J. & Rudd, A. 2015 *Climate hydrology and ecology research support*

system potential evapotranspiration dataset for Great Britain (1961–2015)[CHESS-PE].

Smith, A., Bates, P., Freer, J. & Wetterhall, F. 2014 Investigating the application of climate models in flood projection across the UK. *Hydrological processes* **28**, 2810–2823.

Solander, K. C. & Wilson, C. J. 2018 *The Cape Town drought: what is happening and will it happen again?*. Los Alamos National Lab. (LANL), Los Alamos, NM, United States.

Tanguy, M., Dixon, H., Prosdocimi, I., Morris, D. & Keller, V. 2016 Gridded estimates of daily and monthly areal rainfall for the United Kingdom (1890–2015)[CEH-GEAR]. *NERC Environmental Information Data Centre*. https://doi.org/10.5285/33604ea0-c238-4488-813d-0ad9ab7c51ca.

Taylor, V., Chappells, H., Medd, W. & Trentmann, F. 2009 Drought is normal: the socio-technical evolution of drought and water demand in England and Wales, 1893–2006. *Journal of Historical Geography* **35**, 568–591.

Thornthwaite, C. W. 1948 An approach toward a rational classification of climate. *Geographical review* **38**, 55–94.

Tirivarombo, S., Osupile, D. & Eliasson, P. 2018 Drought monitoring and analysis: Standardised Precipitation Evapotranspiration Index (SPEI) and Standardised Precipitation Index (SPI). *Physics and Chemistry of the Earth, Parts A/B/C* **106**, 1–10.

Tsakiris, G., Pangalou, D. & Vangelis, H. 2007 Regional drought assessment based on the Reconnaissance Drought Index (RDI). *Water resources management* **21**, 821–833.

Van Loon, A. & Laaha, G. 2015 Hydrological drought severity explained by climate and catchment characteristics. *Journal of Hydrology* **526**, 3–14.

Vangelis, H., Tigkas, D. & Tsakiris, G. 2013 The effect of PET method on Reconnaissance Drought Index (RDI) calculation. *Journal of Arid Environments* **88**, 130–140.

Watts, G., Battarbee, R. W., Bloomfield, J. P., Crossman, J., Daccache, A., Durance, I., Elliott, J. A., Garner, G., Hannaford, J. & Hannah, D. M. 2015 Climate change and water in the UK–past changes and future prospects. *Progress in Physical Geography* **39**, 6–28.

Weatherhead, E. & Howden, N. 2009 The relationship between land use and surface water resources in the UK. *Land Use Policy* **26**, S243–S250.

Weatherhead, E. & Knox, J. 2000 Predicting and mapping the future demand for irrigation water in England and Wales. *Agricultural Water Management* **43**, 203–218.

Zarch, M. A. A., Sivakumar, B. & Sharma, A. 2015 Droughts in a warming climate: A global assessment of Standardized precipitation index (SPI) and Reconnaissance drought index (RDI). *Journal of Hydrology* **526**, 183–195.

First received 15 June 2019; accepted in revised form 29 February 2020. Available online 1 April 2020